PROCEEDINGS OF SCIENCE

Searches for Dark Matter with CMS

Sudha Ahuja[*†] **on behalf of the CMS Collaboration**
UNESP - Universidade Estadual Paulista (BR)
E-mail: sudha.ahuja@cern.ch

A summary of the current status of dark matter searches from the CMS experiment is presented, using up to 35.9 fb^{-1} of data collected at 13 TeV in 2016. Various analyses covering mono-object searches along with searches for dark matter mediators are presented. The results are interpreted using simplified models for dark matter.

Sixth Annual Conference on Large Hadron Collider Physics (LHCP2018)
4-9 June 2018
Bologna, Italy

[*] Speaker.

[†] This material is based upon work supported by the Sao Paulo Research Foundation (FAPESP) under Grant No. 2013/01907-0.

PoS(LHCP2018)284

1. Introduction

Dark matter (DM) searches are explored by both astrophysics and particle physics. While its existence has already been inferred by various astrophysical observations [1], there exists no strong evidence to establish the nature of this elusive form of matter. According to recent observations from Planck collaboration [2], most of the energy budget of the universe consists of unknown entities with $\sim 26.8\%$ being dark matter. Dark matter is inferred to exist from gravitational effects on visible matter, being undetectable by emitted or scattered electromagnetic radiation. The hunt for dark matter is being pursued by several types of experiments, mainly classified as direct detection, indirect detection and collider searches. Many extentions of the standard model provide candidates for dark matter. DM candidates are a prime feature of theories predicting weakly interacting particles producing missing energy signals at particle colliders, particularly Supersymmetry, and models with extra dimensions.

DM interactions have been approximated using the effective field theory (EFT) approach that integrates out the details of the mediator. Many Run 1 results from ATLAS and CMS collaborations used the EFT approach for DM data analysis and intepretations. However, the EFT approach uses the contact interaction approximation, has limited scope and ceases to be valid when the energy of the DM interactions is near or above the mass of the mediator(s). Recently, simplified models [3] have become a more popular way for interpreting the DM results. They are able to describe the full kinematics of DM production at the LHC and allow for a comparison of DM particle properties to the direct detection experiments. They involve various parameters that characterize the dark matter particles and their coupling to the visible particles. A massive spin-0 (scalar or pseudoscalar particle) or spin-1 (vector or axial-vector particle) boson mediates the interaction between the standard model (SM) and the DM particles and produces a pair of DM particles. The searches for DM production at colliders focus on collisions with a large transverse momentum imbalance coming from DM particles recoiling against some initial state radiation (X) which could be a gluon, photon or a weak gauge boson Z, W. These searches can also be termed as Mono-X searches.

The searches presented in this document are performed using up to 35.9 fb^{-1} of 13 TeV pp collision data collected by CMS in 2016. The detailed description of the CMS detector can be found in Ref.[4]. The CMS particle-flow (PF) algorithm [5] is used to reconstruct and identify each particle using the optimized set of combined information from the sub-detectors.

2. Mono-X Searches

Monojet/V: The monojet search [6] uses final states with a large missing transverse momentum recoiling against one or more energetic jets. The jets result from the fragmentation and hadronization of quarks or gluons produced in the hard scattering process as initial-state radiation or as the decay products of a vector boson V (W or Z). Thus, the search is referred to as monojet or mono-V search. The Feynman diagrams for the monojet and the mono-V processes are shown in Figure 1.

The results are interpreted in terms of simplified DM models, along with fermion portal DM model, light nonthermal DM model, and the Arkani-Hamed–Dimopoulos–Dvali (ADD) model.

Signal extraction is performed using the distribution of p_T imbalance in each event category. Events in data are selected using triggers based on the $p_{T,trig}^{miss}$ (magnitude of the vector $\vec{p}_T$ sum of all PF candidates at trigger level) and $H_{T,trig}^{miss}$ (magnitude of the vector $\vec{p}_T$ sum of jets with $p_T > 20$ GeV and $|\eta| < 5.0$) thresholds. Candidate events are selected with $p_T^{miss} > 250$ GeV, and the leading AK4 (AK8) p_T jet requirement as $p_T > 100$ GeV (250 GeV) for the monojet (mono-V) category. Jets in the events are reconstructed by clustering PF candidates using the anti-k_T (AK) algorithm [7] and with a distance parameter of 0.4 and 0.8 for the AK4 and AK8 jets respectively. The missing transverse momentum (p_T^{miss}) is derived from the magnitude of the negative vector sum of transverse momenta of all PF candidates in the event. The main backgrounds for this search come from Z($\nu\nu$)+jets (largest background contribution) and W($l\nu$)+jets processes. Background events from Z+jets, W+jets, top-quark pairs ($t\bar{t}$) are reduced by vetoing events with prompt, isolated leptons (electrons, muon or tau leptons), isolated photons, and b-tagged jets. For the mono-V category, the jet coming from the hadronic decays of Lorentz-boosted W or Z bosons are required to have jet mass between 65 and 105 GeV. Further, to distinguish boosted jets from the ones coming from light quarks or gluons, a N-subjettiness [8] variable (τ_N) is employed such that the ratio, τ_2/τ_1, is less than 0.6. The main backgrounds are estimated by performing a simultaneous fit over several control regions (CRs) in data. Data are found to be in agreement with the SM prediction. Figure 2 (left) shows the p_T^{miss} distributions for the monojet category for the signal region (SR). Results are interpreted in terms of DM models assuming a vector, axial-vector, scalar, or pseudoscalar mediator [3] with mass m_{med}. Figure 2 (middle and right) shows the exclusion limits for the vector and axial-vector mediators in the $m_{med} - m_{DM}$ plane.

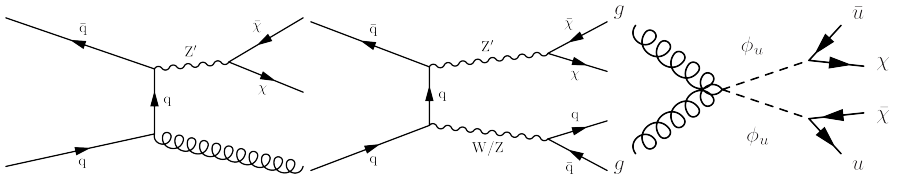

Figure 1: Feynman diagrams for the production mechanisms of DM particles through the monojet, mono-V and the multijet (Fermion portal model) signatures [6].

Mono-Z (leptonic): The signature in this analysis [9] comes from the production of a pair of leptons, originating from a Z boson, together with large p_T^{miss}. SM processes coming from ZZ and WZ serve as the main backgrounds to the analysis, along with WW, leptonically decaying top quark processes, Drell-Yan production, and tri-boson processes. Online events are selected using di-lepton triggers. Events are required to have two well-identified, isolated opposite sign and exactly two same flavour leptons (e or μ). The dilepton pair invariant mass is required to be within the 15 GeV Z boson mass window and with $p_T > 60$ GeV to reject the bulk of low p_T background. Events with more than one jet, at least one b-tagged jet and with additional leptons are vetoed. Further, to obtain the best signal sensitivity, an optimized selection is applied based on the following variables: $p_T^{miss} > 100$ GeV, $\Delta\phi(\vec{p}_T^{ll}, \vec{p}_T^{miss}) > 2.6$ rad and $|p_T^{miss} - p_T^{ll}|/p_T^{ll} < 0.4$. Dominant background contributions are estimated using the simultaneous maximum likelihood fit to the combined information from simulation and the CRs in data. Figure 3 (left) shows the p_T^{miss} in the ee + $\mu\mu$ channel in the SR. No deviation from the SM background expectation is found. Figure 3 (middle and right) shows the 95% confidence level (CL) expected and observed limits for vector

and axial-vector scenarios with couplings $g_q = 0.25$, $g_{DM} = 1$.

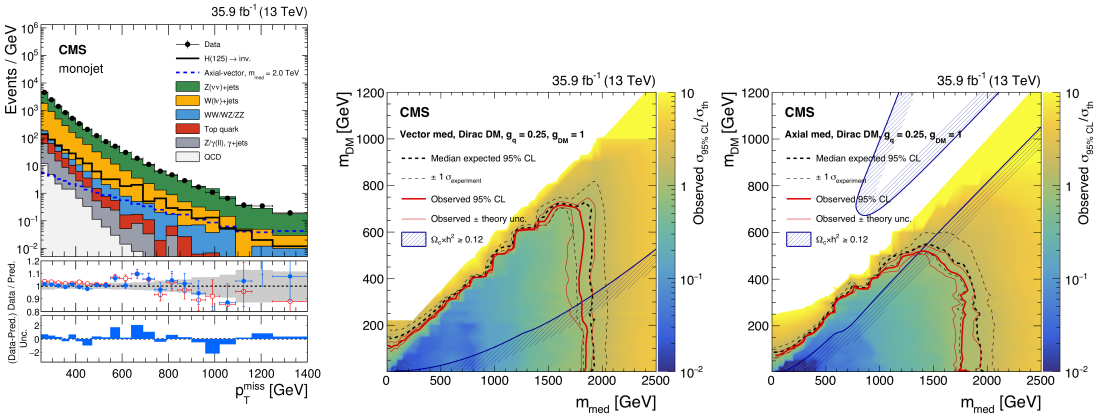

Figure 2: Left: Comparison between the observed p_T^{miss} distribution and the background predictions in the SR, obtained from a combined fit performed in all CRs for the monojet category. Middle and right: Exclusion contours in the $m_{med} - m_{DM}$ plane for the vector (middle) and axial-vector (right) mediators [6].

Mono-top (hadronic): The search [10] uses events with $p_T^{miss} > 250$ GeV, along with a hadronically decaying Lorentz boosted top quark, where the top quark decays to a bottom and a W, with W decaying to two light quarks. Hadronized light quarks or gluons are reconstructed with the anti-k_T algorithm [7]. However, the signature of the boosted top quark is reconstructed using Cambrige-Aachen algorithm [11] with a distance parameter of 1.5 (CA15) where one of the subjets is required to be b-tagged. Further, the PUPPI algorithm [12] and the softdrop grooming method [13] are used to deal with pileup subtraction and to remove soft and wide-angle radiation inside jets. A boosted decision tree (BDT) discriminator (Fig. 4 (left)) based on the three classes of substructure observables, N-subjettiness variable (τ_N) [8], HEPTOPTAGGERV2 [14], and the energy correlation functions (ECF) [15], are used to discriminate top-quark jets from single light quarks and gluons. Backgrounds events come from processes such as pair production of top quarks, W $\rightarrow \ell\nu$ and Z $\rightarrow \nu\nu$ with large p_T^{miss}. Events with at least one well identified and isolated lepton or photon are vetoed in order to suppress the backgrounds. A simultaneous binned likelihood fit over the p_T^{recoil} (p_T of recoiling jets) distribution in all the signal and control regions is performed. The CR predictions are translated to the SR through transfer factors. The final results are interpreted in terms of simplified models for monotop production via flavor-changing neutral current [10] as seen in Figure 4 (middle) for the vector mediator case in a 2D plane defined by the mediator and the DM masses.

DM with top-quark pairs: This search [16] covers three decay modes of $t\bar{t}$ production: all hadronic, lepton+jets (l = e or μ), and dileptonic (ee, eμ, $\mu\mu$). The background is dominated by $t\bar{t}$ and V+jets (V = W, Z/γ^*) production. Several CRs enriched in the standard model processes are used to improve background estimates for the all-hadronic and l+jets SRs and a simultaneous fit over p_T^{miss} distributions is used to extract the DM signal. Dark matter production in association with $t\bar{t}$ offers better search sensitivity in comparison to other modes produced in association with a jet, and the all-hadronic channel provides the best sensitivity. Figure 4 (right) shows the exclusion limits on the signal strength as a function of mediator and dark matter masses, assuming a scalar mediator.

Mono-Higgs ($\gamma\gamma$, $\tau\tau$): The search [17] considers the DM recoiling against a SM-like Higgs boson and with Higgs decaying to the $\tau\tau$ and $\gamma\gamma$ in the final state. Two benchmark simplified models, Z'-two-Higgs-doublet model (Z'-2HDM) [18] and the Z' baryonic model [19] are considered to describe the DM+h production (Fig. 5). While the h $\rightarrow$ b$\bar{\text{b}}$ channel has the highest branching fraction, the $\gamma\gamma$ decay offers a higher precision in reconstructed invariant mass while the $\tau\tau$ channel benefits from a smaller SM background. The largest background contributions to the $\gamma\gamma$ channel come from the non-resonant $\gamma\gamma$, γ+jet, and QCD multijet production, while backgrounds to the $\tau\tau$ channel are from the W + jets, t$\bar{\text{t}}$ and the multijets processes. For the $\gamma\gamma$ channel, a fit to the diphoton invariant mass is performed to extract the signal and background yields. Events are selected using diphoton triggers with photons selected using a loose selection criteria. The diphoton invariant mass is required to be greater than 95 GeV, and the events are further categorized into high-p_T^{miss} ($\geq$ 130 GeV and $p_T^{\gamma\gamma} > 90$ GeV) and low-p_T^{miss} ($50 < p_T^{miss} < 130$ GeV and $p_T^{\gamma\gamma} > 75$ GeV). Further background rejection is achieved by using topological conditions: $|\Delta\phi(p_{\gamma\gamma}, p_T^{miss})| > 2.1$ and $\min(|\Delta\phi(p_{jet}, p_T^{miss})|) > 0.5$. For the $\tau\tau$ channel, the three final states eτ_h, $\mu\tau_h$ and $\tau_h\tau_h$ (where e/μ - leptonic and τ_h - hadronic decays of τ) are considered for the analysis. Single lepton or triggers with two isolated τ_h candidates are used to select the events. For the eτ_h, $\mu\tau_h$ channels, the e and μ are selected using a multivariate MVA discriminator and an isolation requirement. Hadronically decaying τ are required to satisfy loose ($\tau_h\tau_h$ channel) or tight (eτ_h,$\mu\tau_h$ channels) selections. Further selections include: $p_T^{miss} > 105$ GeV, $p_T^{\tau\tau} > 65$ GeV, mass($\tau\tau$ system) < 125 GeV (compatible with SM Higgs) and $\Delta R(\tau\tau) < 2.0$. Further, events with b-tagged jets or with additional leptons are vetoed. Finally, the signal extraction is performed using maximum-likelihood fit to the total transverse mass distributions in the different channels for the SR, and for the W+jets and QCD multijet background CRs. The exclusion contours for the Z'-2HDM model for the combination of both $\gamma\gamma$ and $\tau\tau$ channels can be seen in Figure 5 (right).

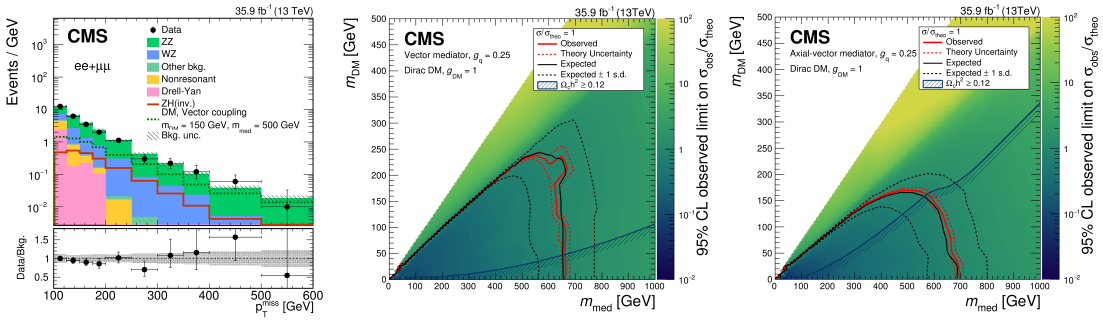

Figure 3: Results for the Mono-Z (leptonic) analysis [9].

3. Mediator Searches

In models with DM particles coupling to quarks through a DM mediator, the mediator can either decay to pair of DM particles or a pair of quarks, which can be observed as a dijet resonance. The resonance can be broad or narrow, depending on the strength of the coupling. Following the recommendations of the LHC DM working group [20], we consider DM simplified models with a spin-1 mediator decaying only to q$\bar{\text{q}}$ and pairs of DM particles, with an unknown mass and a universal quark coupling $g_q = 0.25$ and a DM coupling $g_{DM} = 1.0$.

Dijet Resonance Search: The search [21] is performed for both broad and narrow resonances scenarios. The narrow resonance search is conducted for both low mass (0.6 – 1.6 TeV) and high mass (> 1.6 TeV) categories. The limits are used to constrain simplified models of DM, with leptophobic vector and axial-vector mediators that couple only to quarks and DM particles. Figure 6 (left) shows the excluded region of mediator mass (m_{med}) as a function of DM mass (m_{DM}) for the axial-vector mediator. The exclusions are also compared to constraints from the cosmological relic density of DM determined from astrophysical measurements [22].

Dijet Angular Analysis: The angular distribution of dijets relative to the beam direction is sensitive to the dynamics of the scattering process. The angular distributions of the dominant underlying QCD processes are all similar and there is no strong dependence on the parton distribution functions (PDFs). Dijet angular distributions are measured in terms of $\chi_{\text{dijet}} = \exp(|y_1 - y_2|)$, where y_1 and y_2 are the rapidities of the two highest p_T jets. Beyond SM processes may have scattering angle distributions that are closer to being isotropic than those given by QCD processes and can be identified by an excess of events at small values of χ_{dijet}. Figure 6 (middle) shows the normalized χ_{dijet} distributions [23] unfolded to particle level and compared to various DM signal distributions for a particular dijet mass bin.

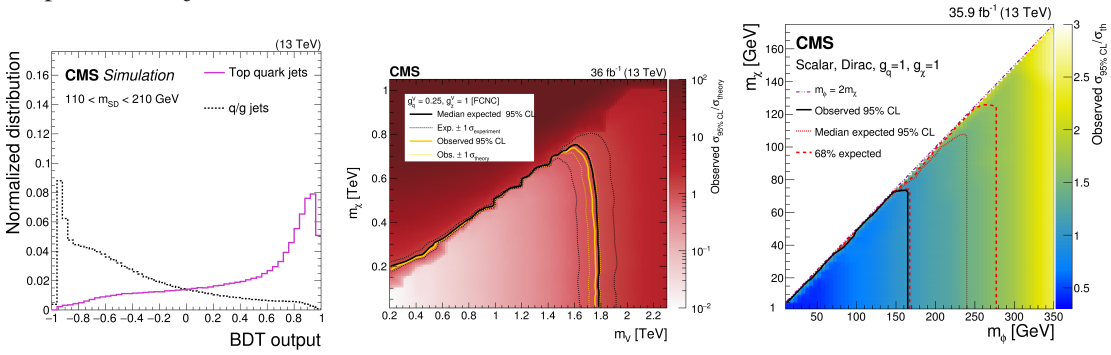

Figure 4: Results from the Mono-Top (hadronic) [10] and the DM+$t\bar{t}$ analyses [16].

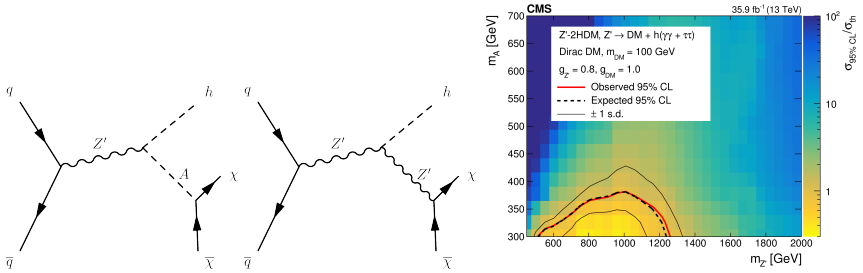

Figure 5: Feynman diagrams and results for the Mono-Higgs analysis [17].

4. Conclusion

The CMS DM searches presented cover various final states and scenarios, leading to stringent constraints on the existence of weakly interacting particles. The results are interpreted using the simplified models for dark matter that include different possible types of interactions between DM and SM particles. No significant excess was observed compared to SM backgrounds and the results were used to set exclusion limits on various new physics models.

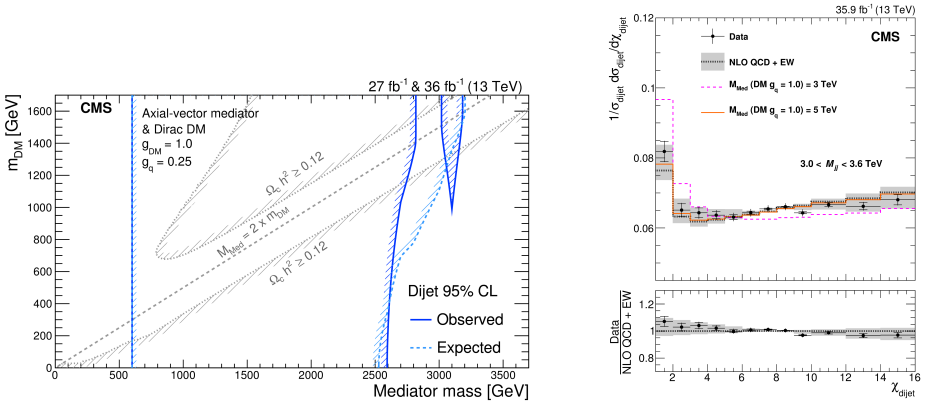

Figure 6: Results from dijet resonance analyses [21][23] .

References

[1] G. Bertone, D. Hooper, and J. Silk, Phys. Rept. 405 (2005) 279.

[2] Planck Collaboration, A&A 594, A13 (2016).

[3] O. Buchmueller, M. J. Dolan, and C. McCabe, JHEP 01 (2014) 025.

[4] CMS Collaboration, JINST 3 (2008) S08004.

[5] CMS Collaboration, JINST 12 (2017) P10003.

[6] CMS Collaboration, Phys. Rev. D 97 (2018) 092005.

[7] M. Cacciari, G. P. Salam, and G. Soyez, JHEP 04 (2008) 063.

[8] J. Thaler and K. Van Tilburg, JHEP 03 (2011) 015.

[9] CMS Collaboration, Eur. Phys. J. C 78 (2018) 291.

[10] CMS Collaboration, JHEP 06 (2018) 027.

[11] Y. L. Dokshitzer, G. D. Leder, S. Moretti, and B. R. Webber, JHEP 08 (1997) 001.

[12] D. Bertolini, P. Harris, M. Low, and N. Tran, JHEP 10 (2014) 59.

[13] A. J. Larkoski, S. Marzani, G. Soyez, and J. Thaler, JHEP 05 (2014) 146.

[14] C. Anders et al., Phys. Rev. D 89 (2014) 074047.

[15] A. J. Larkoski, G. P. Salam, and J. Thaler, JHEP 06 (2013) 108.

[16] CMS Collaboration, CMS-EXO-16-049, http://cds.cern.ch/record/2631721.

[17] CMS Collaboration, JHEP 09 (2018) 046.

[18] A. Berlin, T. Lin, and L. Wang, JHEP 78 (2014) 1.

[19] L. Carpenter et al., Phys. Rev. D 89 (2014) 24.

[20] A. Boveia et al., arXiv:1603.04156. J. Abdallah et al., Phys. Dark Univ. 9-10 (2015) 8.

[21] CMS Collaboration, JHEP 08 (2018) 130.

[22] D. N. Spergel et al., Astrophys. J. Suppl. 170 (2007) 377. Planck Collaboration, A&A 571 (2014) A16.

[23] CMS Collaboration, CMS-EXO-16-046, http://cds.cern.ch/record/2309935.